Available online at www.sciencedirect.com
SCIENCE DIRECT
Journal of Catalysis 239 (2006) 51–64
JOURNAL OF CATALYSIS
www.elsevier.com/locate/jcat

Reduction of stored NO_x on Pt/Al_2O_3 and $Pt/BaO/Al_2O_3$ catalysts with H_2 and CO

Tamás Szailer [a], Ja Hun Kwak [a], Do Heui Kim [a], Jonathan C. Hanson [b], Charles H.F. Peden [a], János Szanyi [a,*]

[a] *Institute for Interfacial Catalysis, Pacific Northwest National Laboratory, Richland, WA 99352, USA*
[b] *Chemistry Department, Brookhaven National Laboratory, Upton, NY 11973, USA*

Received 1 August 2005; revised 8 December 2005; accepted 4 January 2006

Available online 9 February 2006

Abstract

In situ Fourier transform infrared spectroscopy, coupled with mass spectrometry and time-resolved X-ray diffraction, were used to study the efficiency of nitrate reduction with CO and H_2 on Pt/Al_2O_3 and $Pt/BaO/Al_2O_3$ NO_x storage reduction (NSR) catalysts. Surface nitrates were generated by NO_2 adsorption, and their reduction efficiencies were examined on the catalysts together with the analysis of the gas-phase composition in the presence of the two different reductants. H_2 was found to be a more effective reducing agent than CO. In particular, the reduction of surface nitrates proceeds very efficiently with H_2 even at low temperatures (~420 K). During reduction with CO, isocyanates form and adsorb on the oxide components of the catalyst; however, these surface isocyanates readily react with water to form CO_2 and ammonia. The NH_3 thus formed in turn reacts with stored NO_x at higher temperatures (>473 K) to produce N_2. In the absence of H_2O, the NCO species are stable to high temperatures and are removed from the catalyst only when they react with NO_x thermal decomposition products to form N_2 and CO_2. The results of this study point to a complex reaction mechanism involving the removal of surface oxygen atoms from Pt particles by either H_2 or CO, the direct reduction of stored NO_x with H_2 (low-temperature NO_x reduction), the formation and subsequent hydrolysis of NCO species, and the direct reaction of NCO with decomposing NO_x (high-temperature NO_x reduction).

Keywords: NO_x reduction; Reduction efficiency; Pt/Al_2O_3; $Pt/BaO/Al_2O_3$; FTIR; TR-XRD

1. Introduction

Improving the fuel economy of internal combustion engines is critically needed in a world of declining oil reserves. Engines operating under net oxidizing conditions (e.g., diesel engines) exhibit better fuel efficiency than those operating under stoichiometric air/fuel ratios. As a result of these fuel-"lean" operating conditions, however, traditional three-way catalysts are unable to reduce the emission of harmful NO_x gases to the low levels required by environmental regulations. In the presence of excess oxygen, these catalysts oxidize all of the reducing agents present in the exhaust stream (H_2, CO, and hydrocarbons), thus starving the catalyst for an efficient reductant. In the past decade, a number of technologies have been considered for NO_x reduction in net oxidizing environments. Among these technologies, plasma-assisted NO_x reduction [1], selective catalytic reduction (SCR) by hydrocarbons [2,3] and by urea [4], and NO_x storage-reduction (NSR) catalysis [3] have yielded the most promising results.

An NSR catalyst contains a noble metal (usually Pt or Rh), and a storage material (most commonly BaO) on an alumina support. The role of the noble metal constituent is twofold: to oxidize NO (the main NO_x in the exhaust stream) to NO_2 in the lean cycle, and to reduce NO_x in the rich cycle. These systems can operate only under cyclic conditions; that is, a NO_x storage period (net oxidizing conditions) must be followed by a brief reduction step (net reducing conditions) [5]. The main findings of numerous reports on recent NO_x reduction research have been summarized in a review by Burch [3]. Most of the studies in this field have focused on the NO_x adsorption and

* Corresponding author.
E-mail address: janos.szanyi@pnl.gov (J. Szanyi).

0021-9517/$ – see front matter
doi:10.1016/j.jcat.2006.01.014

storage processes, with the reduction step receiving considerably less attention.

Lesage et al. [6] studied the NO_x trap mechanism by Fourier transform infrared (FTIR) spectroscopy on a $Pt/BaO/Al_2O_3$ catalyst. They examined the reduction efficiencies of H_2 and CO under flow conditions and found that H_2 was a much better reducing agent than CO. They also observed the formation of two types of surface NCO species during the reduction cycle with CO. These NCO species were shown to react readily with O_2 or H_2O, forming $N_2 + CO_2$ and $NH_3 + CO_2$, respectively. In fact, the hydrolysis of surface NCO species with H_2O has been well established on Pt/Al_2O_3 catalysts, even at room temperature [7].

The reduction efficiency of different reducing agents was also studied by Jozsa et al. [8] on a commercial $Pt/BaO/Al_2O_3$ NO_x storage/reduction catalyst. In temperature-programmed reduction experiments with H_2, CO, or C_3H_6, these authors found that H_2 was the most effective agent for the reduction of stored NO_x. Similar conclusions were reached by Poulston and Rajaram [9] and James et al. [10] on $Pt/BaO/Al_2O_3$-based NO_x storage materials.

Cant and Patterson [11] investigated the reduction efficiencies of different reducing agents for samples without precious-metal components. They exposed a BaO/Al_2O_3 storage material at 300 °C to a flow of 1000 ppm NO_2 and 3% O_2. In the reduction cycle under dry conditions, quite contrary to other results, CO was found to be a more effective reductant on BaO/Al_2O_3 than H_2. These findings may relate to the absence of a noble metal in the catalyst formulation, which is essential for the activation of H_2.

Under practical conditions, both CO and H_2 are available for NO_x reduction. In the present study, we addressed the interaction of CO and H_2 reducing gases with NO_x species formed in the adsorption of NO_2 on Pt/Al_2O_3 and $Pt/BaO/Al_2O_3$ catalysts. We identified surface species formed in the reaction of H_2 and CO with adsorbed NO_x using IR spectroscopy and followed the composition of the gas phase by mass spectrometry during the course of the reduction. The information obtained from these experiments has provided useful insights into the complex reaction mechanism of NO_x reduction over these catalysts.

2. Experimental

The catalysts were prepared by the incipient wetness method, using aqueous $Ba(NO_3)_2$ (Aldrich) and dinitrodiammine platinum (Aldrich) solutions to impregnate γ-alumina supports (Condea, 200 m^2/g). The impregnation was carried out in sequential manner. The alumina support was first impregnated with the $Ba(NO_3)_2$ solution, then with the Pt-containing solution. The final loading was 2.5 wt% for the Pt/Al_2O_3 catalyst and 2 wt% Pt and 20 wt% BaO for the $Pt/BaO/Al_2O_3$ catalyst. After impregnation, the catalysts were dried at 395 K and then calcined at 773 K in a flowing 5% O_2/He gas mixture for 2 h. This procedure ensured the decomposition of essentially all of the precursor $Ba(NO_3)_2$ phase into BaO. The Pt dispersions for these two catalysts (as determined by H_2 chemisorption and TEM) were very similar, ∼45–50%.

The IR measurements were carried out in transmission mode, using a Nicolet Magna-IR 750 spectrometer operating at 4 cm^{-1} resolution. Before acquisition of each spectral series, a background spectrum of the clean, adsorbate-free sample was obtained. The IR cell was a 2-$\frac{3}{4}''$ six-way stainless steel cube equipped with CaF_2 windows. The cell was connected to a gas handling/pumping station and through both leak and gate valves to a mass spectrometer (UTI 100C). The catalyst sample was pressed onto a fine tungsten mesh, which was mounted onto a copper sample holder assembly attached to ceramic feedthroughs of a 2-$\frac{3}{4}''$ flange. This setup allowed us to heat the samples to 1000 K and to subsequently cool the samples to cryogenic temperatures. The sample temperature was monitored through a chromel/alumel thermocouple spot-welded to the top center of the tungsten mesh. Before NO_2 adsorption, the samples were reduced with H_2 at 573 K.

The nitrate species were always generated on the Pt/Al_2O_3 and $Pt/BaO/Al_2O_3$ catalysts by NO_2 adsorption. The reduction of stored NO_x was carried out with H_2, CO, or $H_2 + CO$. After NO_2 adsorption at room temperature, the chamber was evacuated and the reductant was introduced. In the presence of reductant, the catalyst was heated at a rate of 12 K/min to the desired temperature, maintained at that temperature for 1 min, and then cooled back to room temperature. (In some of the experiments, IR spectra were also recorded at the reaction temperature.) After 5 min thermal equilibration time, IR and mass spectra were collected. The catalyst was once again heated, and the entire procedure was repeated generally until a temperature of 573 K was reached. After the final reduction step was completed, the chamber was evacuated, and temperature-programmed desorption (TPD) was carried out at a heating rate of 12 K/min. During the course of the TPD experiments, IR spectra were collected at selected sample temperatures.

The reduction of NO_x species on a $Pt/BaO/Al_2O_3$ catalyst was also studied with time-resolved X-ray diffraction (TR-XRD). The TR-XRD experiments were carried out at beam line X7B of the National Synchrotron Light Source at Brookhaven National Laboratory. The sample was exposed to a constant NO_2 flow, using a 250-ppm NO_2/He gas mixture, and heated from 300 to 573 K. After completion of the NO_2 adsorption at 573 K, the sample was cooled to 300 K in flowing NO_2 and purged with He. The changes in the crystalline $Ba(NO_3)_2$ phase during the reduction with H_2 (5% H_2 in He) and CO (5% CO in He) were then studied with TR-XRD as the sample was heated in accordance with a designed temperature program to 573 K under the flowing reductant.

3. Results and discussion

3.1. Pt/Al_2O_3

As we have discussed previously [12], the alumina support material that was not completely covered by the Ba-containing active NO_x storage phase can store NO_x in the form of surface nitrates when exposed to NO_2 up to temperatures relevant to NO_x storage/reduction catalysis. Therefore, we first investigated the reduction process of adsorbed NO_x species on a

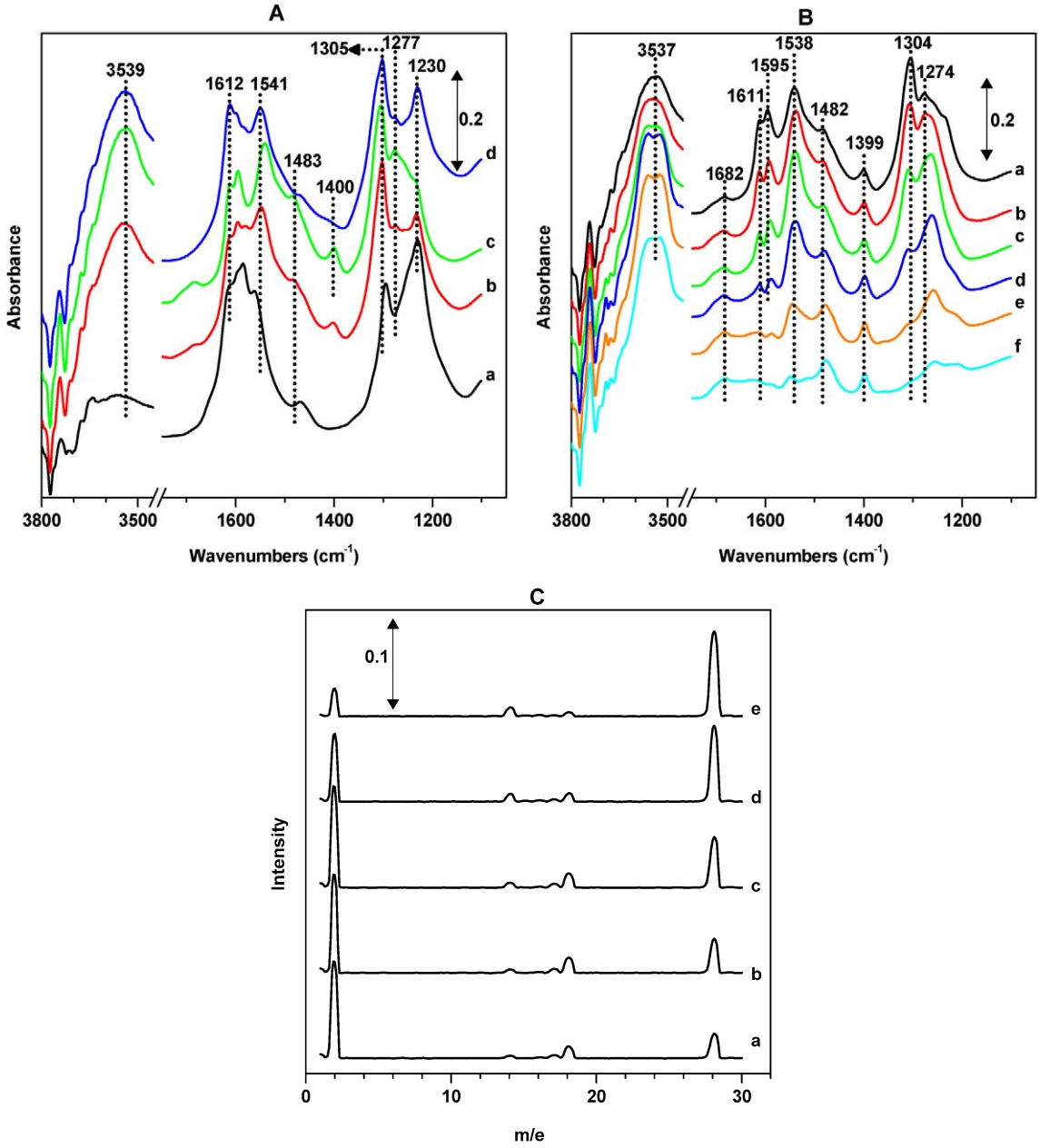

Fig. 1. Reduction of NO_x with H_2 on Pt/Al_2O_3. (A) IR spectra: NO_2 adsorption (a), followed by H_2 exposure for 2 (b) and 60 min (c) at 300 K, or by H_2O adsorption at 300 K (d). (B) IR spectra: after NO_2 and H_2 exposures at room temperature (a) and at 373 K (b), 423 K (c), 473 K (d), 523 K (e), 573 K (f). (C) Mass spectra corresponding to IR spectra b → f in panel (B).

Pt/Al_2O_3 catalyst with both H_2 and CO. Surface nitrates were generated on a 2.5 wt% Pt/Al_2O_3 catalyst by exposure to 5 Torr of NO_2 at room temperature (spectrum a in Fig. 1A). The resulting IR bands can be assigned to different types of nitrates formed on the alumina support: bridging (1606–1630 cm^{-1} and 1211–1266 cm^{-1}), bidentate (1571–1612 cm^{-1} and 1249–1293 cm^{-1}), monodentate (1575–1588 and 1292–1297 cm^{-1}), and linear (1479 cm^{-1}), according to previously reported results [13,14].

3.1.1. Reduction with H_2

After NO_2 adsorption, the sample was exposed to H_2 in an amount greater than needed for the complete reduction of NO_x species just formed on the Pt/Al_2O_3 catalyst. The changes in the IR spectra as a function of time during the reduction process with H_2 at room temperature are shown in Fig. 1A (spectra b and c). In the presence of H_2, significant changes in the IR spectra were observed even at 300 K. Specifically, a broad peak in the OH region at ∼3540 cm^{-1} grew continuously with time-on-stream, indicating the formation of water. This water was most likely produced by the removal of adsorbed oxygen atoms from the surfaces of Pt particles with H_2. These oxygen atoms were generated on the Pt particles when the catalyst was exposed to NO_2. In fact, XPS results by Olsson and Fridell [15] showed that Pt can be oxidized to platinum oxides (PtO_2 and PtO) during NO_2 adsorption on Pt/Al_2O_3 or $Pt/BaO/Al_2O_3$ catalysts.

For comparison, spectrum d of Fig. 1A shows the effect of 5 Torr H_2O on the IR spectra of the freshly nitrated sample. The intensity of the 3540-cm^{-1} IR feature produced by interaction of H_2O with the NO_x-covered alumina surface is very close to that produced during the reduction with H_2. Close inspection of the spectral region between 1200 and 1800 cm^{-1} allows us to distinguish between the effects on the stored NO_x by interaction with water or by reduction with H_2. The IR features in the 1480–1620 cm^{-1} region and the peak at 1305 cm^{-1} show very similar behavior in the presence of either H_2 or H_2O. This suggests that these peaks are influenced primarily by water formed in the reduction by H_2. The peak at 1400 cm^{-1} was observed only in the presence of H_2; this peak was assigned by Westerberg and Fridell [14] to the formation of bulk nitrates. The results of our recent combined FTIR/TR-XRD studies clearly indicate the formation of bulk nitrates from surface nitrates in the presence of water vapor [16]. The introduction of H_2 reduced the intensity of the 1230 cm^{-1} peak and increased the intensity of the 1305, 1541, and 1612 cm^{-1} peaks. In addition, a new feature developed at ∼1280 cm^{-1}. Some of these observations can be rationalized by the formation of nitrites (N-coordinated, 1538 cm^{-1}; linear, 1485 cm^{-1} [14]) as H_2 interacts with the nitrate species.

A series of FTIR spectra obtained during reduction with H_2 at different sample temperatures are presented on Fig. 1B. The reactivity of the different bidentate (surface) nitrates (bridging, 1610 and 1260 cm^{-1}; chelating, 1595 and 1305 cm^{-1}) was much higher than that of the bulk-type nitrates (1399 cm^{-1}), which remained unchanged during the reduction up to 573 K. The linear nitrites (1482 cm^{-1}) were more stable toward reduction with H_2 than the N-coordinated nitrites (1538 cm^{-1}). The intensity of this latter peak increased up to 423 K, possibly due to H_2O formation, as discussed earlier. The surface concentration of H_2O maximized at 473 K, as evidenced by the highest intensity of the 3537-cm^{-1} IR feature. Subsequently, the intensity of this peak decreased due to water desorption from the catalyst at these elevated temperatures.

The gas-phase products of NO_x reduction with H_2 were N_2 and water. A series of mass spectra obtained after each elevated temperature excursion, followed by room temperature equilibration, is shown in Fig. 1C. From the mass spectra shown, it is clear that with increasing sample temperature, the extent of NO_x reduction increases, as evidenced by the increasing concentration of N_2 in the gas phase (28 amu), as well as the simultaneous decrease in the concentration of H_2, the reductant. The seemingly decreasing level of H_2O in the gas phase after elevated temperature reactions (>473 K) is most likely a result of water readsorption on the catalyst surface, along with decreasing partial pressure of water in the gas phase in the IR cell due to the formation of large amounts of N_2.

3.1.2. Reduction with CO

The series of experiments described above were also conducted with CO as the reductant. At room temperature, no changes in the IR spectra with time-on-stream were observed. This suggests that CO does not react with surface NO_x species at room temperature. Spectra acquired during reduction of surface nitrates (generated with $^{15}NO_2$) by CO at elevated temperatures are shown in Fig. 2A. At room temperature, a small IR feature of Pt-adsorbed CO appeared at 2083 cm^{-1}. The intensity of this peak increased significantly as the sample was heated to 473 K, due to the removal of surface oxygen from the Pt particles. As the sample temperature reached 473 K, surface NCO species began to form (2200–2300 cm^{-1}), and their concentration increased until reaching a maximum at 573 K. Further increases in sample temperature resulted in decreased surface concentration of NCO. The two bands found in this region were assigned to the asymmetric vibration of NCO, bound to octahedral (2260 cm^{-1}) and tetrahedral (2222 cm^{-1}) Al^{3+} sites [7,17,18]. These isocyanate species formed on the Pt particles and spilled over onto the alumina support surface.

Assignment of the IR bands at 1824, 1782, 1643, and 1485–1490 cm^{-1} was aided by comparing the IR spectra recorded at reaction temperatures with those obtained after the sample was cooled to room temperature after the elevated temperature reactions. A series of IR spectra collected at reaction temperatures is shown in Fig. 2B (these spectra were recorded before those shown in Fig. 2A). Comparing the two sets of IR spectra displayed in Figs. 2A and B clearly shows that the spectra collected at elevated temperatures were much simpler than those obtained after thermal equilibration at room temperature after elevated temperature reactions. The IR features that we are trying to assign here (1485–1490, 1643, 1782, and 1824 cm^{-1}) were present only in the spectra collected at room temperature after elevated temperature reactions (>470 K). These IR features represent adsorbed species that are formed in the reduction of surface-bound NO_x species and weakly bonded to the catalyst surface. The bands at 1480–1490 and 1643 cm^{-1} can be assigned to weakly bound surface carbonates formed by the interaction of CO_2, a product of the NO_x reduction with CO, and the alumina support. Assignment of the 1782 and 1824 cm^{-1} IR features is fairly straightforward as well. This spectral region is characteristic of the ν_{N-O} vibration of adsorbed NO on precious metal particles [17]. The presence of NO in the gas phase is evident from the results of mass spectrometry analysis (Fig. 2D). As the reduction of stored NO_x increased with increasing sample temperature, the concentration of gas-phase NO increased as well. Its concentration reached a maximum at 523 K, after which it decreased and completely disappeared by 623 K. In the IR spectra, however, the doublet feature was present at 1782 and 1824 cm^{-1} even after the reduction step at 673 K. A gradual decrease in CO concentration also occurred as the extent of NO_x reduction increased with increasing sample temperature. As the surface of the Pt particles became less populated by adsorbed CO (see Fig. 2A), adsorption sites became available for NO. As CO was consumed in the reduction process, some NO remained in the system that could adsorb on the clean, reduced Pt particles. The 8–10 cm^{-1} isotopic shift (when using $^{15}NO_2$ instead of $^{14}NO_2$) in the positions of these features also support the assignment to adsorbed NO species. A doublet feature in the 1750–1830 cm^{-1} region has also been attributed to adsorbed NO and CO bound to the same iridium [19] or rhodium [20] atom. However, this type of adsorption complex can be ruled

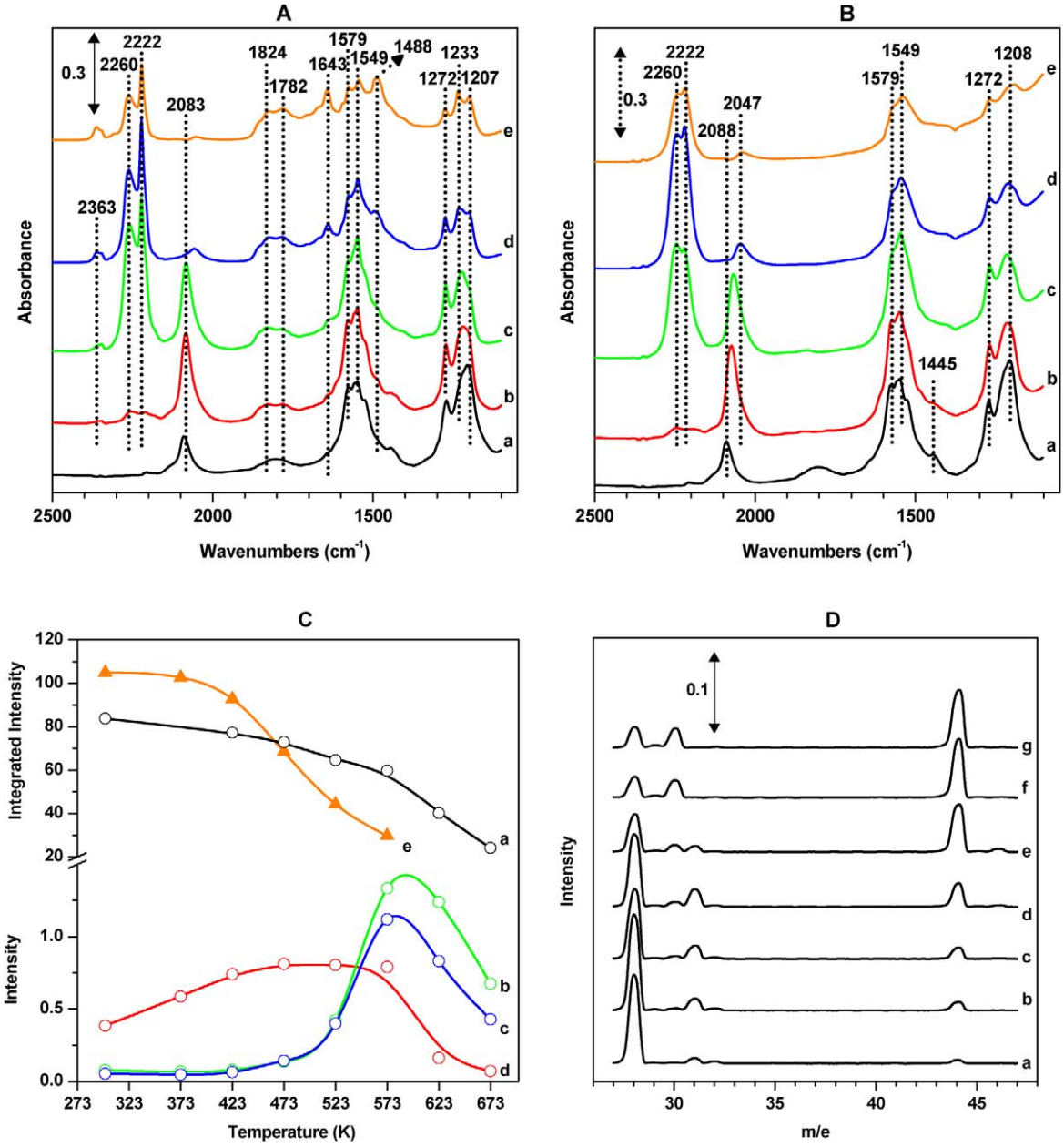

Fig. 2. Reduction of NO_x species on Pt/Al_2O_3. (A) IR spectra after $^{15}NO_2$ and CO adsorption at 300 K (a), and subsequent short (1 min) excursions to 473 K (b), 573 K (c), 623 K (d), and 673 K (e) (spectra taken at room temperature). (B) IR spectra corresponding to those in panel (A), but taken at reaction temperatures. (C) Changes in the surface concentrations of nitrates (a), isocyanates (b and c), and Pt–CO (d) during reduction with CO (the change in the nitrates concentration in the reduction with H_2 is also displayed (e)). (D) Mass spectra after reduction at 373 K (a), 423 K (b), 473 K (c), 523 K (d), 573 K (e), 623 K (f), 673 K (g).

out in our case, because this doublet was present with high intensity even after all CO was consumed.

The intensities of the IR features of selected surface species as a function of sample temperature are displayed in Fig. 2C. These plots provide some insight into the changes in the concentrations of these species, which in turn could aid understanding the mechanism responsible for the reduction of surface NO_x species. They depict the total integrated intensity of the nitrate region and the maximum intensities of the other surface species (adsorbed CO and NCO). For comparison, the figure also shows the integrated intensity of the nitrate region during reduction with H_2. Although Pt/Al_2O_3 was reduced before NO_2 adsorption in each experiment, the intensity of the ν_{CO} band of adsorbed CO increased up to 523 K, suggesting that a large number of Pt sites became accessible at elevated reaction temperatures as the Pt-bound O atoms (formed during NO_2 exposure) were removed. As the catalyst was saturated with CO, the transformation of nitrate species started at 473 K, in concert with NCO formation. The IR results clearly show that the surface concentration of NCO species reached a maximum at around 590 K, then decreased as they were converted to other adsorbed species and/or desorb/decompose. After reduction at the maximum temperature studied (673 K), no adsorbed CO was detected, and the surface concentration of NCO was dra-

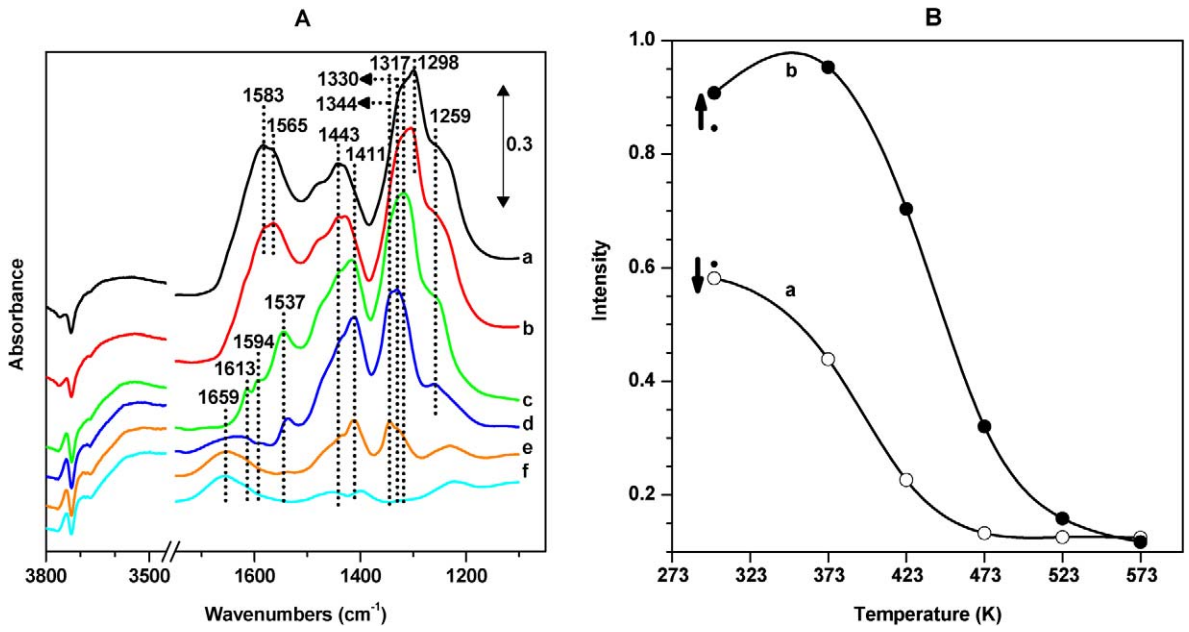

Fig. 3. Reduction of NO_x species with H_2 on $Pt/BaO/Al_2O_3$. (A) NO_2 exposure (a) followed by H_2 adsorption (b) at 300 K, and reduction at 373 K (c), 423 K (d), 473 K (e), 573 K (f). (B) Intensities of the 1580 cm^{-1} (a) and 1330 cm^{-1} (b) IR peaks as a function of reduction temperature (filled symbols refer to peak intensities before H_2 adsorption at 300 K).

matically decreased; however, a significant amount of nitrate species remained on the catalyst surface.

Postreaction gas analysis data are consistent with the results of the IR measurements presented above. A series of mass spectra obtained after heating the sample for 1 min at the indicated temperatures is displayed in Fig. 2D. As the reduction of the NO_x species proceeded, the concentration of gas-phase CO (the reductant) decreased, whereas that of CO_2 increased. The primary N-containing reaction products were $^{15}N_2$ (30 amu) and ^{15}NO (31 amu). Note the formation of a small amount of $^{15}N_2O$ (46 amu), particularly at 573 K.

Comparing the mass spectra with the corresponding IR spectra shows that the concentration of gas-phase CO decreased continuously during NO_x reduction. In good agreement with the IR spectra that showed increased CO coverage on the Pt particles up to 473 K, the gas-phase concentration of CO decreased slightly in this temperature range. Above 473 K, the CO concentration reached a plateau as the appearance of the IR signature of surface NCO species signaled the onset of NO_x reduction. The concentration of gas-phase CO_2 increased slowly up to 473 K, in agreement with the limited extent of NO_x reduction. Above 473 K, the concentration of surface NCO species increased rapidly, reached a maximum at around 590 K, and then decreased. The largest increases in both CO_2 (both gas-phase and surface-bound) and N_2 concentrations, together with the steepest decline in CO concentrations, occurred in the temperature range in which the NCO coverage decreased. These observations seem to indicate a significant role of surface-bound NCO species in the overall reduction mechanism of NO_x species on Pt/Al_2O_3.

Computing the relative decrease in the concentration of nitrate species (with an initial nitrate integrated intensity taken as 100%) from the curves of Fig. 2B revealed that H_2 was a more effective reducing agent (72% reduction) than CO (26% reduction) at 573 K. The significant difference in reduction efficiency, together with the formation of a significant amount of NCO species on the catalyst surface during the reduction of NO_x with CO, suggest differing reduction mechanisms for H_2 and CO. In the IR experiments, two different types of NCO species assigned to different alumina sites were formed. These NCO species were strongly adsorbed onto the catalyst surface, making their removal quite difficult. In a postreaction TPD experiment, the NCO-related IR features disappeared at high temperature (650 K), where the decomposition of the unreacted nitrate species also occurs. We propose that at these high temperatures, the thermally released NO_x converted the NCO to CO_2 and N_2 (and/or N_2O). In fact, in the TPD spectrum we observed the formation of N_2O, together with NO, in the temperature range where the IR features of adsorbed NCO decreased and the nitrate features disappeared. Based on the strong adsorption of NCO, one might predict that NCO can poison the catalyst. Although this might be the case in these experiments, under practical operations, NCO can be hydrolyzed in the presence of H_2O (see later) to form NH_3 and CO_2, or oxidized with the large excess of oxygen present in the exhaust gas stream.

3.2. *Pt/BaO/Al$_2$O$_3$*

To generate adsorbed NO_x species, the catalyst was first exposed to 10 Torr of NO_2 at 300 K. The 1100–1800 cm^{-1} and 3500–3800 cm^{-1} spectral regions of the IR spectrum recorded after NO_2 exposures of the $Pt/BaO/Al_2O_3$ catalyst at 300 K are shown in Fig. 3A (spectrum a). The absorption features are very similar to those reported previously by us [12] and others [21–24] for BaO/Al_2O_3 and $Pt/BaO/Al_2O_3$ systems. In accordance with our previous findings [12], even at this relatively

high BaO content (20 wt%), we can still observe NO_x species adsorbed onto the alumina support surface (IR bands at 1230–1259 and 1594–1613 cm^{-1}), although at low coverages. The most intense IR features, however, are those representing nitrate species associated with the presence of the BaO phase on the alumina support, that is, surface (bidentate) nitrates (1298 and 1583 cm^{-1}) and bulk (ionic) nitrates (1317 and 1400–1480 cm^{-1}). Following the generation of nitrate species on the catalyst, we investigated their reduction using H_2 and then CO as reducing agents.

3.2.1. Reduction with H_2

A series of IR spectra obtained during the course of reduction with H_2 at different sample temperatures (300–573 K) is displayed in Fig. 3A (spectra b–f). When hydrogen was introduced onto the catalyst with preadsorbed NO_x at room temperature, small changes in the intensities of the IR features were observed; bands assigned to surface nitrates (1298 and 1583 cm^{-1}) decreased slightly, whereas the two bands of bulk nitrates (1443 and 1300 cm^{-1}) increased marginally. These changes became more pronounced when the sample was gradually heated up to higher temperatures. Whereas the intensities of the surface nitrate features decreased continuously, those of the bulk nitrates reached a maximum at 373 K, then began to decrease with further temperature increases (Fig. 3B). In particular, the decrease in all of the nitrate features accelerated at temperatures above 373 K. The IR spectra presented in Fig. 3A indicate that surface nitrates on BaO and alumina-bound nitrates are removed most rapidly, followed by the reduction of bulk $Ba(NO_3)_2$. Under the conditions of this experiment, all of the NO_x species formed on the $Pt/BaO/Al_2O_3$ catalyst on NO_2 exposure at 300 K were reduced after the sample was heated to 573 K for 1 min.

The series of IR spectra in Fig. 3 also shows the development of a band at ∼1660 cm^{-1} that can be assigned to the $\delta_{H–O–H}$ vibration of adsorbed water. The formation of water in the reduction of NO_x species on $Pt/BaO/Al_2O_3$ with H_2 may explain the different trends in the reaction pattern of surface and bulk nitrates [16]. As water is formed in the reduction, it interacts strongly with the exposed Al_2O_3 surface and may force the thin Ba-nitrate layer on the alumina support to form bulk nitrates. As a result, the intensities of the bulk nitrate features increase at the beginning of the reduction process. Then, as the extent of reduction increases, these bulk nitrates are reduced at an increasing rate as the sample temperature is raised. The effect of water on the NO_x reduction process on $Pt/BaO/Al_2O_3$ LNT catalysts was studied by Epling et al. [25], who found that in the presence of H_2O, the adsorption of NO_x on alumina was significantly inhibited due to the formation of hydroxyl groups on the alumina surface. Consistent with this are the results of our recent combined ^{15}N solid-state NMR, FTIR, and TR-XRD study revealing that the surface nitrate species on alumina disappeared after the NO_2-saturated BaO/Al_2O_3 sample was exposed to H_2O [12].

3.2.2. Reduction with CO

A series of IR spectra recorded during the reduction of adsorbed NO_x with CO on a $Pt/BaO/Al_2O_3$ catalyst is displayed in Fig. 4A as a function of sample temperature (with $^{15}NO_2$ used for the generation of NO_x species). The IR spectrum (a) obtained after $^{15}NO_2$ saturation and evacuation exhibited the typical nitrate features that we discussed earlier. Interestingly, again we still see some of the features corresponding to adsorption of NO_x species onto the alumina support material, although the BaO coverage was significantly higher than needed to cover the entire support surface. After the introduction of CO at 300 K, no change in the IR spectrum occurred in the nitrate region. A small IR band appeared at 2084 cm^{-1} that we previously assigned to the ν_{CO} vibration of CO linearly adsorbed onto reduced Pt sites. The low CO coverage can be attributed to the oxidation of Pt particles by NO_2 before CO exposure (as we discussed earlier for the Pt/Al_2O_3 system) and/or the partial coverage of Pt particles by the Ba-containing phase. As the sample temperature increased to 373 K and then up to 523 K, the intensity of the Pt-adsorbed CO band increased, although the gas-phase concentration of CO decreased due to the reduction of NO_x. After the highest temperature reduction step (573 K), only a very low intensity feature of adsorbed CO was seen on the Pt particles, because most CO was consumed by NO_x reduction. The 2348 cm^{-1} IR feature of weakly adsorbed CO_2 gradually increased with increasing reduction temperature, in accordance with the increasing extent of NO_x reduction.

Similar to the reduction of NO_x species with CO on the Pt/Al_2O_3 catalyst that we discussed previously (Fig. 2), here the formation of surface-bound NCO species occurred in the 2150–2280 cm^{-1} region. The formation of adsorbed NCO set in at around 423 K, and its concentration increased rapidly as the sample temperature was raised, reaching its maximum intensity at 523 K. Further increasing the sample temperature to 573 K resulted in decreased intensity of the NCO features. Comparing these NCO features obtained on $Pt/BaO/Al_2O_3$ to those seen on the Pt/Al_2O_3 catalysts shows the presence of an additional band in the BaO-containing catalyst at 2158 cm^{-1}, which we assign to NCO species adsorbed onto BaO. (The fact that this band appeared at 2167 cm^{-1} when the NO_x species were generated with NO_2 instead of $^{15}NO_2$ proves that this band also belongs to a NCO vibration. The 9-cm^{-1} frequency shift is in accordance with substitution of ^{15}N for ^{14}N in NCO.)

It is also interesting to note that the relative intensity of the ∼2260 cm^{-1} NCO feature is smaller on $Pt/BaO/Al_2O_3$ than on Pt/Al_2O_3, suggesting that the ratio of octahedral-to-terahedral Al^{3+} sites available for NCO adsorption is modified by the presence of BaO. The highest intensity NCO feature on the Al_2O_3 is the tetrahedral Al^{3+}-bound one. These results suggest that as Ba-nitrates (surface and bulk) are converted to carbonates during the reduction process (or even during the NO_2 adsorption), morphological changes of the Ba-containing phase may open up the alumina support surface for NCO adsorption. The significant intensity of the alumina-bound NCO feature suggests that a large fraction of the Al_2O_3 surface becomes exposed during the reduction with CO. It is also possible that the strong interaction between the NCO species and the alu-

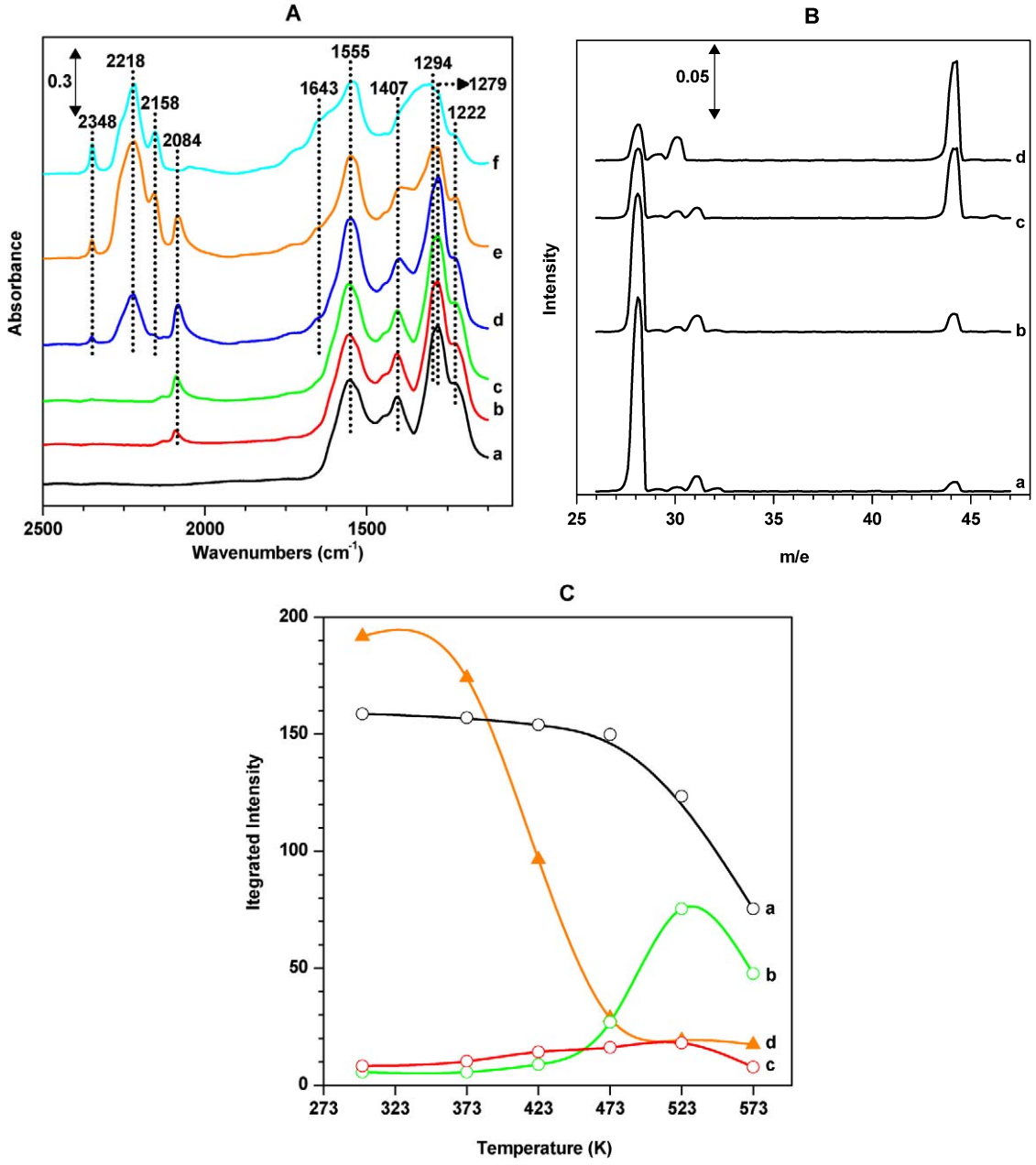

Fig. 4. Reduction of NO_x species with CO on $Pt/BaO/Al_2O_3$. (A) IR spectra after $^{15}NO_2$ (a) followed by CO (b) exposure at 300 K, 373 K (c), 473 K (d), 523 K (e), 573 K (f). (B) Mass spectra after reduction steps at 423 K (a), 473 K (b), 523 K (c), 573 K (d). (C) Integrated intensities of IR bands of surface species: nitrates (a), Pt–CO (c) and isocyanates (b) (for comparison, the integrated intensities of nitrate species during the reduction with H_2 is shown as well (d)).

mina support is the driving force behind these changes. Lesage et al. [6] reported the formation of NCO species in the rich cycle of LNT processes on $Pt/BaO/Al_2O_3$ catalysts using IR spectroscopy in a mechanistic study on a $Pt–Rh/BaO/Al_2O_3$ catalyst. They reported the formation of NCO species bound to Al^{3+} and Ba^{2+} cations during the reduction cycle, although (due to the low intensities of the NCO features) the peak assignments were not without ambiguity. In our experiments, assignment of the three different NCO bands is straightforward.

Mass spectra taken after each elevated temperature reduction step are displayed in Fig. 4B. The gradual intensity decrease of the 28-amu signal clearly indicates the consumption of CO in the reduction process, in agreement with the results of the IR measurements. At the same time, an increased CO_2 concentration in the gas-phase was observed as CO was converted to CO_2. A small amount of NO was also seen at 423 K, but its concentration decreased during the reduction at higher temperatures, and no detectable NO remained after reduction at the highest temperature (573 K). The N_2 concentration gradually increased with increasing reduction temperature and reached a maximum at 573 K. The formation of N_2O was also seen at intermediate reduction temperatures (particularly at 523 K); however, its concentration was very low throughout these experiments.

The integrated IR intensities of nitrates, adsorbed CO, and isocyanates are plotted in Fig. 4C as a function of sample tem-

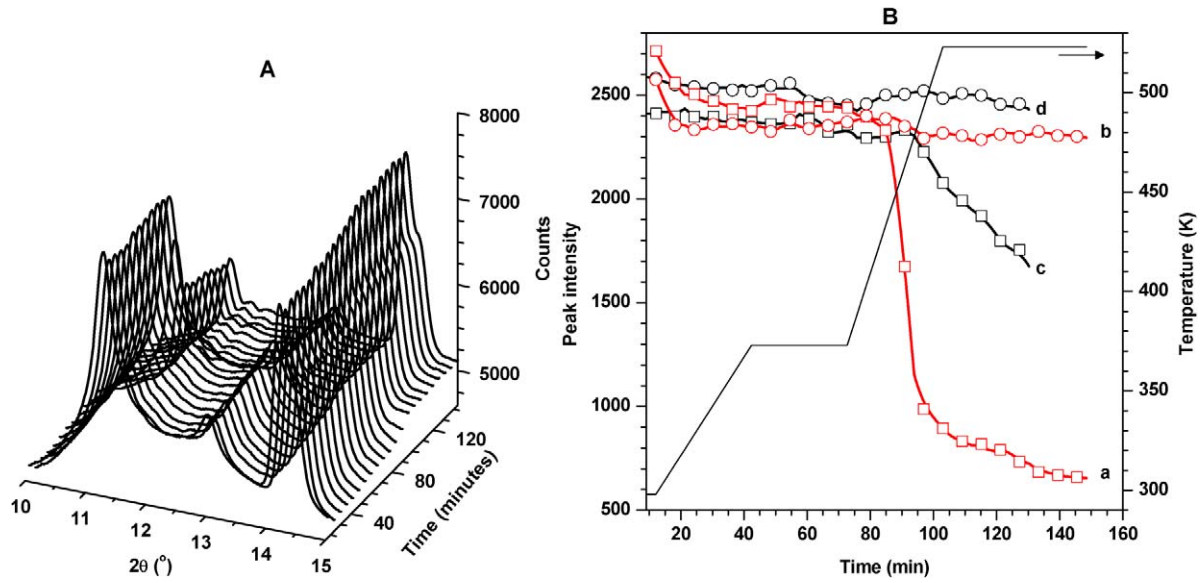

Fig. 5. (A) TR-XRD spectra collected during the reduction of NO_x species with H_2 on $Pt/BaO/Al_2O_3$. (B) The intensities of the (111) diffraction peaks of Ba-nitrate (squares) and Ba-carbonate (circles) species during the reduction of NO_x species with H_2 (red) and CO (black).

perature. For comparison, the integrated intensities of nitrate species during the reduction with H_2 are also shown. The trends in these plots are very similar to those for the reduction of nitrates in Pt/Al_2O_3 that we discussed earlier. The figure clearly shows the difference in reduction efficiency between H_2 and CO. The reduction of nitrates begins just above room temperature and proceeds rapidly above 373 K when H_2 is used as a reducing agent. In contrast, the reduction of nitrates with appreciable rate starts at above 473 K when CO is the reducing agent. It is also worth mentioning that after reduction at 573 K, 78% of the nitrates were removed with H_2 as the reductant, as opposed to 32% with CO as the reductant.

The difference in nitrate reduction efficiencies between H_2 and CO over $Pt/BaO/Al_2O_3$ was also confirmed in TR-XRD experiments. In this study, a constant flow of CO or H_2 was passed through the NO_2-saturated catalyst bed while XRD patterns were acquired during temperature-programmed reductions. The results of these experiments are summarized in Fig. 5. A series of XRD patterns recorded during the reduction process with hydrogen on a $Pt/BaO/Al_2O_3$ sample as a function of time is shown in Fig. 5A, and the temperature profile as a function of time is displayed in Fig. 5B. The changes in the intensities of the (111) Ba-nitrate and the (111) Ba-carbonate peaks are shown as functions of time in the temperature-programmed reduction experiments. In accordance with the IR results discussed above, the decrease in the nitrate phase sets in at a reduction temperature about 100 K lower (∼373 K) with H_2 as the reductant. It is also interesting to note that the rate of reduction of the nitrate phase is much faster with H_2 than with CO, once again confirming the IR results. Furthermore, an increase in the carbonate phase is observed when CO is used as the reducing agent, whereas a small reduction in the carbonate phase occurs for H_2 reduction. The presence of carbonates during the TR-XRD experiments is a result of exposing the catalyst sample to air during sample loading and the subsequent inadequate in situ reduction in the XRD cell. The presence of these carbonates does not alter the main conclusions of this study, however, because only nitrates are reduced in the reduction experiments, and the carbonates are practically just spectators under these conditions (maximum temperature, 500 K).

A TPD experiment was carried out on the $Pt/BaO/Al_2O_3$ sample after reduction of the nitrate species with CO, to investigate the thermal stabilities of species remaining on the catalysts after the reduction cycle. The TPD spectra for selected masses (B) and the IR spectra (A) collected during the TPD run are displayed in Fig. 6. Up to 500 K, the only change observed in both the IR and TPD spectra was the desorption of weakly held CO_2 and carbonates from the oxides (disappearance of the shoulder at around 1645 cm^{-1} in the IR spectrum and a desorption profile centered at around 350 K in the TPD). Above 500 K, a very broad and intense CO_2 desorption feature developed in the TPD spectrum (mass 44), signaling the decomposition of more strongly bound carbonates. The fact that N_2O appeared in the TPD spectra at the same temperature at which CO_2 began to evolve, also coincident with a decreased intensity of the NCO species in the IR spectra, suggests that surface NO_x reacted with NCO present in high coverage on the catalysts. At these temperatures (∼630 K), this reaction produced primarily CO_2 and N_2, and N_2O formation reached a maximum. With further temperature increases, the production of nitrogen increased sharply and the NCO features in the IR spectra decreased dramatically.

We propose that in this temperature regime, nitrates began to decompose thermally and reacted with NCO species to produce N_2 and CO_2. Desorption of NO was delayed compared with that of N_2, presumably due to the initial complete consumption of the desorbed NO_x species in the reaction with NCO. However, as the rate of N_2 evolution reached a maximum, the NO desorption rate increased, as a consequence of the increased NO_x desorption rate at higher temperatures as well as the reduced

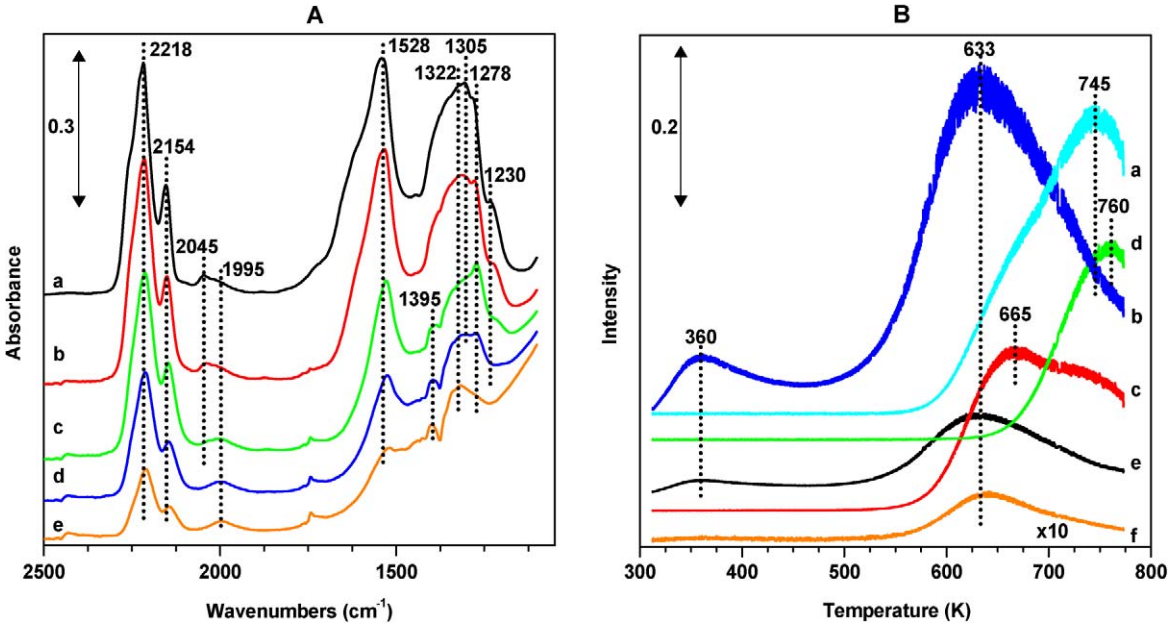

Fig. 6. Post-reduction (with CO) TPD on $Pt/BaO/Al_2O_3$. (A) IR spectra collected at 300 K (a), 500 K (b), 650 K (c), 700 K (d), 750 K (e). (B) TPD profiles for NO (a), CO_2 (b), N_2 (c), O_2 (d), CO (e), and N_2O (f).

concentration of NCO on the catalyst surface. Interestingly, N_2 formation did not cease even at the highest temperature (773 K), in accordance with the continued presence of some NCO on the catalyst surface as evidenced from the IR spectra.

To further rationalize the change in "selectivity" from N_2O to N_2 during these TPD experiments, we note that the small amount of N_2O during the TPD run with a maximum rate at around 640 K likely is a consequence of the relatively high surface coverage of NO on the Pt particles in this temperature regime. As adsorbed NO_x from the Ba-containing phase begins to thermally decompose, it spills over to the Pt particles, where it can decompose to N_a and O_a. At the high surface coverage of NO_a and the low coverage of N_a, there is a relatively high probability of the formation of N_2O by the combination of N_a and NO_a [26]. At higher temperatures, however, N_2O formation slows while N_2 formation speeds up, because the NO_a dissociation rate is more rapid and the lifetime of NO_a is shorter. At even higher temperatures (>700 K), NO desorbs from the catalyst before it can dissociate, resulting in decreased N_2 formation.

In the reduction experiments with CO on both Pt/Al_2O_3 and $Pt/BaO/Al_2O_3$ catalysts, we observed the formation of NCO species with high surface coverage on the oxide components of the catalyst systems BaO and Al_2O_3. As we mentioned in the Introduction, the formation of NCO species during the reduction of NO_x species with CO was reported previously [6,7]. We also noted that these NCO species were easily removed by hydrolysis with water, which is always present in high concentrations (∼10 vol%) in the exhaust gas stream in both lean and rich cycles.

To evaluate the hydrothermal stability of the NCO species generated in the reaction of stored NO_x with CO on the $Pt/BaO/Al_2O_3$ catalysts, we generated NCO species by reacting the adsorbed NO_x (formed via NO_2 uptake) with CO at 523 K. This temperature was chosen because we have observed the highest concentration of surface NCO species after reduction of NO_x with CO at this temperature (see Fig. 4). After 3 min of reduction with CO at 523 K, the catalyst was cooled to room temperature, and the cell was evacuated before H_2O introduction. After the IR spectrum shown in Fig. 7A (a) was obtained, 10 Torr of H_2O was added to the reaction cell, and the sample was heated to increasingly higher temperatures. After each elevated temperature excursion, the catalyst was cooled to room temperature before an IR spectrum was acquired. A mass spectrum was also acquired after each reaction run, to monitor changes in the gas-phase composition.

A series of IR spectra (Fig. 7A) as a function of sample temperature, along with the corresponding mass spectra (B), are displayed in Fig. 7. The mass spectra were collected using $^{15}NO_2$ to generate the surface nitrate species. After the introduction of water at 300 K, the IR feature at 2233 cm^{-1}, representing NCO bound to the tetrahedral aluminum sites, decreased significantly. Changes in the nitrate region are also seen, in accordance with those in the effect of water on adsorbed nitrates that we discussed previously (Fig. 1). The strong interaction between the alumina support and water is the driving force behind the decreased intensity of alumina-bound NCO. From the data shown here, it is not possible to determine whether Al^{3+}...NCO reacted with H_2O at 300 K to form CO_2 and NH_3 or whether it was just replaced by water and forms HNCO and Al^{3+}...OH. The formation of hydroxyl groups was evidenced by the development of a broad ν_{OH} feature above 3500 cm^{-1}; however, no trace of HNCO could be seen in the mass spectrum. In the IR spectra, on the other hand, two new features appeared at 1459 and 1614 cm^{-1}. The intensities of these two features increased significantly as the sample was heated to higher temperatures and reached their maxima

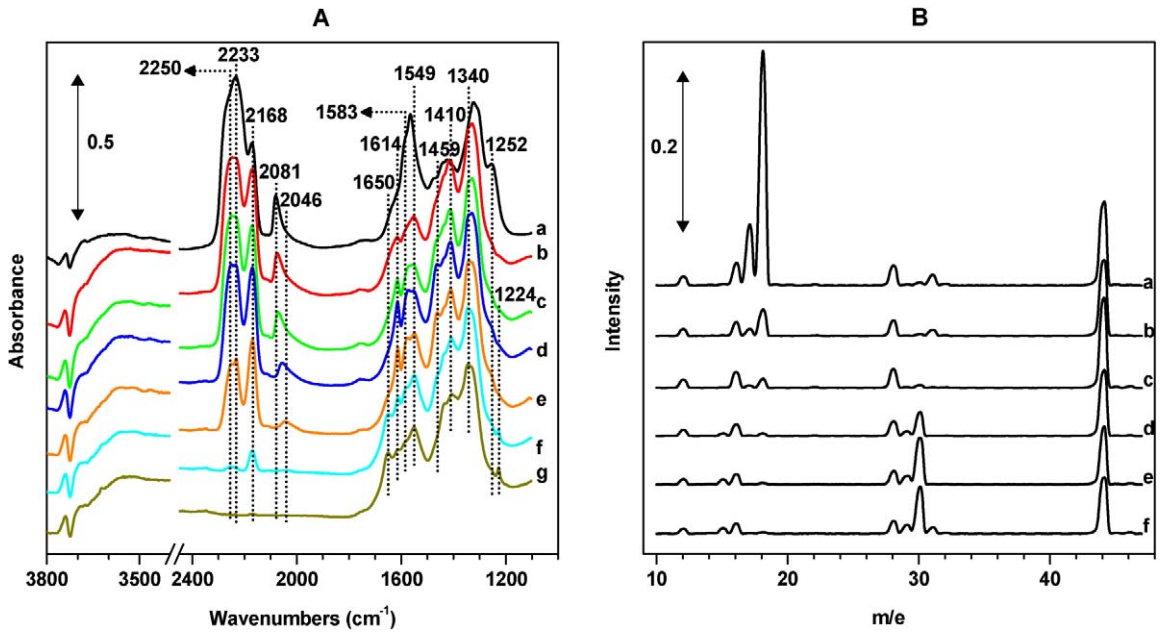

Fig. 7. (A) IR spectra from Pt/BaO/Al_2O_3 after 10 Torr NO_2 and 20 Torr CO exposures followed by heating at 523 K for 3 min (a), and in the presence of 10 Torr H_2O at room temperature (b) and then gradually heated to 373 K (c), 423 K (d), 473 K (e), 523 K (f), and 573 K (g). (B) Mass spectra ($^{15}NO_2$) of the gas phase obtained during reaction at 373 K (a), 423 K (b), 473 K (c), 523 K (d), 573 K (1 min) (e), and 573 K (10 min) (f).

at 473 K. These peaks can be assigned to Lewis acid-bound (1614 cm^{-1}) and protonated (1459 cm^{-1}) NH_3.

Interestingly, after the significantly decreased intensity of the tetrahedral Al^{3+}-bound NCO feature (2233 cm^{-1}), the intensities of octahedral Al^{3+}-bound NCO species decreased as the sample was heated to 423 K. Note that there was no change in the intensity of the Ba-bound NCO species in this temperature range. Heating the sample to 473 K resulted in a decrease in all three NCO bands. As the sample temperature reached 523 K, most of the alumina-bound NCO features disappeared, and only a small trace of the Ba-bound NCO remained. Above 473 K, the intensities of the NH_3-related bands (1614 and 1459 cm^{-1}) also decreased, due to either the desorption of these species or their reaction with NO_x species still present in the catalyst. The results of this experiment clearly demonstrate the facile reaction between NCO formed in the reaction of stored NO_x and CO with water to form ammonia by hydrolysis. The significantly different reactivities of these NCO species toward hydrolysis are also evident. The series of mass spectra shown in Fig. 7B demonstrate a gradual consumption of H_2O as the hydrolysis of the NCO species proceeds with increasing rate as the sample temperature is raised. Also note the formation of a large amount of N_2 above 473 K (mass 30). At lower temperatures (<473 K), as the NCO species are hydrolyzed, NH_3 remains mostly adsorbed on the catalyst surface. At higher temperatures, however, it can react with stored NO_x to produce N_2.

3.2.3. *Reduction with CO + H_2*

Because under practical operating conditions, both H_2 and CO are present in the exhaust gas stream, we investigated the reduction of nitrate species on a Pt/BaO/Al_2O_3 catalyst in the presence of both reductants at various temperatures. After cooling the sample to 300 K following each 1-min reduction step at the indicated temperature, we collected a series of IR and mass spectra, as displayed in Fig. 8. As in previous experiments, we generated the nitrate species by exposing the catalyst to NO_2 at 300 K and then evacuating the IR cell. The IR spectrum recorded after NO_2 adsorption was identical to that discussed earlier and showed the presence of typical nitrate features (spectrum a) (nitrates on the alumina support and the surface and bulk nitrates in the BaO phase). Exposure of this NO_2-saturated sample to an equimolar H_2 + CO gas mixture for 60 min (spectrum b) did not appreciably change the IR spectrum other than the appearance of one additional feature at 2089 cm^{-1} representing CO adsorbed onto metallic Pt sites. Although the greatest amount of CO was available for adsorption under these conditions, the IR peak of adsorbed CO was weak, almost certainly due (as discussed above) to the oxidation of surface Pt sites by NO_2 in the previous step, in which the nitrate species were generated. In fact, it is conceivable that most of the surface Pt sites are oxidized, and hence CO can adsorb only on Pt sites that have been freed through the removal of O_a by either of the reducing agents present (as H_2O with H_2 or CO_2 with CO). The appearance of a low-intensity CO_2 feature seems to support this hypothesis.

Heating the sample to 423 K in the CO + H_2 mixture did not affect the IR spectrum in the nitrate region, whereas a significant increase in the intensity of the Pt-bound CO feature occurred (spectrum d), and the CO_2 band increased as well. The alumina-bound NCO features were of much higher intensity than the Ba-related NCO. (Most of the Ba^{2+} ions are associated with NO_x species, with only a limited amount of BaO available for NCO adsorption.) Further increasing the sample temperature to 473 K resulted in both the disappearance of the Pt-bound CO feature and intensity gains in all three adsorbed NCO features (spectrum e). The intensities of the NCO features dropped

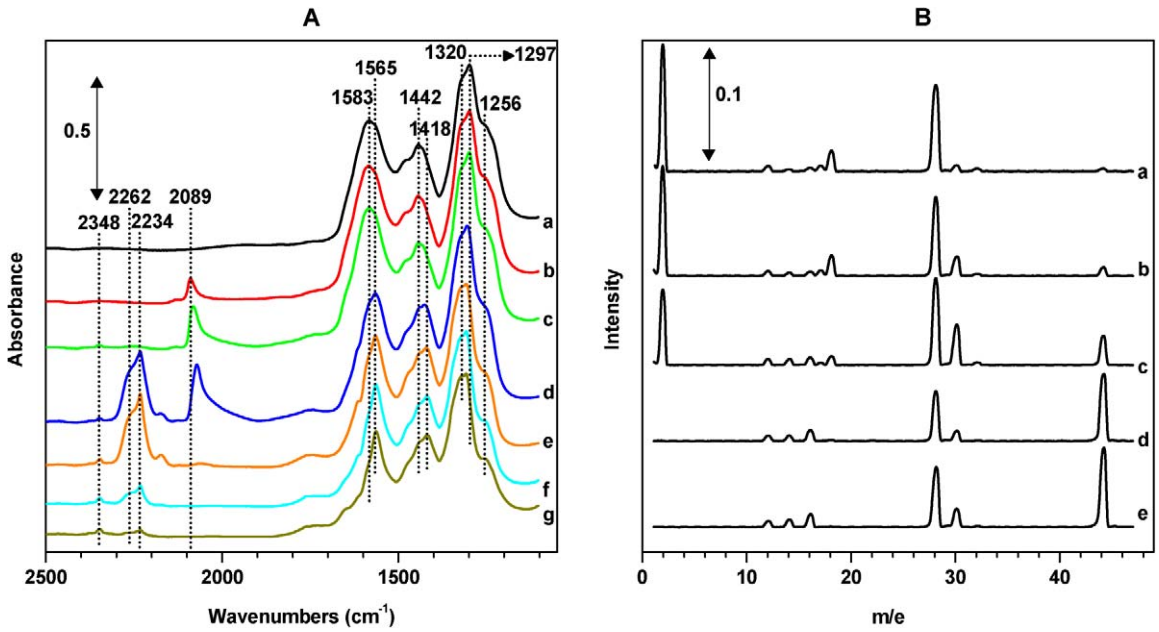

Fig. 8. (A) IR spectra from Pt/BaO/Al_2O_3 after exposure to 10 Torr NO_2 (a) followed by 5 Torr CO and 5 Torr H_2 adsorption at room temperature for 60 min (b), and then gradually heated to 373 K (c), 423 K (d), 473 K (e), 523 K (f), and 573 K (g). (B) Corresponding mass spectra after reduction at room temperature (for 60 min) (a), 373 K (b), 423 K (c), 473 K (d), and 573 K (e).

dramatically as the sample was heated to 523 K (spectrum f) and subsequently to 573 K (spectrum g).

Evaluating the mass spectra obtained after each reduction step at elevated temperatures may provide insight into the changes observed in the IR spectra of Fig. 8A. After the NO_2-saturated catalyst was exposed to the CO + H_2 gas mixture at 300 K for 60 min, hydrogen and CO were the dominant components of the mass spectrum (spectrum a). Small amounts of water and CO_2 were also seen, in agreement with the results of the IR experiment, suggesting that reaction occurs (albeit to a limited extent) even at room temperature. At 373 K, more N_2 and CO_2 formed, whereas the concentrations of H_2 and H_2O seemed to remain unchanged. As we discussed previously for the reduction of NO_x species with H_2 only on the Pt/BaO/Al_2O_3 catalyst, at 373 K some of the nitrates (particularly the surface nitrates) already exhibited reduction. The mass spectrum collected after reduction at 423 K (spectrum c) shows significant decreases in the concentrations of both H_2 and H_2O in the reactant/product gas mixture, along with rapid increases in the concentrations of N_2 and CO_2 formed in the reduction. As the concentrations of H_2 and H_2O dropped, the intensity of the NCO feature in the IR spectrum rapidly increased (spectrum d in Fig. 8A), and the surface CO concentration reached a maximum; however, the NCO concentration was much lower than that occurring when CO was the only reductant (Fig. 4). After reduction at 473 K, neither H_2 nor H_2O was present in the gas phase, and the amount of remaining gas-phase CO was minimal. In fact, no (or hardly any) Pt-bound CO was observed in the IR spectrum after this reduction step, suggesting that practically all of the CO reductant had been consumed by reactions producing NCO or CO_2. After the reduction at 573 K, the primary constituents of the gas mixture in the reaction cell were N_2 and CO_2, and the IR spectrum exhibited almost complete disappearance of the NCO features.

3.3. Reduction mechanisms with H_2 and CO

The mechanistic picture that emerges from the results of these experiments can be characterized as follows. In the presence of H_2 only, hydrogen was activated on the Pt surface and first reacted with the O_a remaining on the Pt surface from the reaction of NO_2 with the catalyst (the reverse reaction of NO oxidation to NO_2 over Pt in a NO + O_2 mixture), forming water,

$$\mathrm{Pt}\ldots\mathrm{O_a} + \mathrm{H_2} \rightarrow \mathrm{Pt^*} + \mathrm{H_2O}, \quad (1)$$

where Pt* denotes empty Pt sites. The H_2O thus formed destabilized some of the adsorbed nitrates, particularly surface nitrates on alumina, which could then decompose on the Pt surface. The dissociation of NO_x species on the Pt particles can be followed by the recombination of N_a atoms to form N_2 or by the reaction of these N_a atoms with H_2 to form NH_x and, ultimately, NH_3,

$$2\mathrm{Pt}\ldots\mathrm{N_a} \rightarrow 2\mathrm{Pt^*} + \mathrm{N_2} \quad (2)$$

and

$$(x+1)\mathrm{Pt^*} + \mathrm{NO}_x \rightarrow x\,\mathrm{Pt}\ldots\mathrm{O_a} + \mathrm{Pt}\ldots\mathrm{N_a}. \quad (3)$$

Thus, in this process the primary role of H_2 is to keep the surfaces of the Pt particles clean for the dissociation of NO_x by reacting with O_a to form H_2O [reaction (1)]. It also has been suggested that H_a promotes NO dissociation on Pt catalysts [27]. Pirug and Bonzel [28] reported decreased activation energy for NO dissociation with decreasing NO coverage and proposed that coadsorbed hydrogen can prevent high NO coverage, thereby enhancing the rate of NO dissociation. Of

course, removing O_a will also facilitate the dissociation of NO by restoring active sites for this part of the process.

In the presence of CO at low temperatures (<423 K), the primary reaction was the removal of adsorbed oxygen atoms (Pt…O_a) from the Pt particles to form CO_2. The empty Pt sites thus formed became available for adsorption of CO, which could then react with adsorbed nitrogen atoms to form NCO species,

$$\mathrm{Pt}\ldots\mathrm{N_a} + \mathrm{Pt}\ldots\mathrm{CO_a} \rightarrow \mathrm{Pt^*} + \mathrm{Pt\text{–}NCO_a}. \quad (4)$$

NCO generated on the Pt particles spilled over to the oxide components of the catalyst, resulting in consumption of a large fraction of the gas-phase CO and formation of a significant amount of CO_2 (Fig. 6B) via

$$\mathrm{Pt}\ldots\mathrm{O_a} + \mathrm{CO} \rightarrow \mathrm{Pt^*} + \mathrm{CO_2}. \quad (5)$$

On the other hand, only a very small amount of N_2 could form via reaction (2), because of the relatively low temperatures (<423 K). Therefore, NCO and CO_2 formation (but not N_2 formation) occurred at the expense of adsorbed nitrate species (stored NO_x). At higher temperatures, these NCO species can readily react with the NO_x stored by the catalyst. The onset of this reaction (>573 K) corresponds with the onset of stored nitrate decomposition. This reaction route eventually led to the disappearances of both nitrate and NCO features in the IR spectra (Fig. 8),

$$\mathrm{NCO_a} + \mathrm{NO}_x \rightarrow \mathrm{N_2} + \mathrm{CO_2}. \quad (6)$$

In fact, we cannot rule out significant N_2 formation at these higher temperatures arising from reaction (2). However, N_2 formation was significantly enhanced by adding water to the NCO-covered catalysts. Adding water opened up a new reaction route for the NCO: the hydrolysis to form NH_3 and CO_2,

$$\mathrm{NCO_a} + \mathrm{H_2O} \rightarrow \mathrm{NH_{2;a}} + \mathrm{CO_2} \quad (7)$$

and

$$\mathrm{NH_{2;a}} + \mathrm{H_2O} \rightarrow \mathrm{NH_3} + \mathrm{OH_a}. \quad (8)$$

The NH_3 thus formed could now react with NO_x to form the intermediate that eventually generated N_2 and H_2O,

$$\mathrm{NH_3} + \mathrm{NO}_x + \mathrm{H_2O} \rightarrow [\mathrm{NH_4NO}_x] \rightarrow \mathrm{N_2} + \mathrm{H_2O}. \quad (9)$$

In the simultaneous presence of both H_2 and CO reducing agents, nitrogen formation was rapid; however, the reaction path cannot be considered to involve merely the simple addition of reactions occurring in the presence of the individual reducing agents. In the low-temperature regime (<373 K), the primary reducing agent was H_2, and the reaction seemed to follow a similar path to that discussed above for the H_2-only case. Nonetheless, the formation of Al_2O_3-bound NCO is more facile at lower temperatures in the presence of H_2 than in the presence of only CO. Salama et al. [29] observed no NCO formation at low temperatures in the CO + NO reaction over an Au/Na-Y catalyst; however, after introducing H_2 to the gas mixture, they observed the development of an intense NCO feature in the IR spectrum suggesting the formation of N_a atoms. They attributed this observation to the promotion of N–O bond fission by adsorbed atomic hydrogen. A similar phenomenon was recently reported by Macloed and Lambert [30] on a Pd/Al_2O_3 catalyst. These authors observed that in the presence of H_2, the N–O and C–O bonds are destabilized in adsorbed NO and CO, respectively, most likely due to the enhanced backdonation from the metal to the antibinding orbitals of NO and CO in the presence of adsorbed hydrogen on the metal surface.

It is reasonable to assume that a similar phenomenon holds for other noble metals as well (although the effect of H_2 on the N–O and C–O bonds likely varies with different noble metals). The rapid accumulation of NCO species on the catalyst surface (seen in the CO-only reduction experiment) was not observed in the presence of both H_2 and CO, because the water produced in the reduction with H_2 efficiently hydrolyzed these adsorbed NCO species. Comparing the results displayed in Figs. 3 and 8 clearly shows that the reduction rate of stored NO_x was lower in the presence of both H_2 and CO than in the presence of only H_2, most likely due to the competition between H_2 and CO for adsorption sites on the Pt particles. This in turn resulted in a lower H_a concentration in the presence of CO, thus effectively reducing the rate of NO_x reduction at low temperature with H_2. On the other hand, NO_x reduction was significantly higher in the presence of both H_2 and CO than with CO only. This is due primarily to the aforementioned reduction in the N–O and C–O bond strengths in the presence of adsorbed hydrogen, as well as to the efficient hydrolysis of surface NCO in the presence of H_2.

4. Conclusion

This study investigated the efficiency of H_2 and CO in the reduction of stored NO_x on Pt/Al_2O_3 and $Pt/BaO/Al_2O_3$ catalysts. Both reducing agents were found to effectively reduce stored NO_x; however, H_2 is a much more effective reductant than CO. H_2 more effectively reduced the surface nitrates than the bulk nitrates on $Pt/BaO/Al_2O_3$. In the reduction with CO (in the absence of H_2O), the formation of isocyanates bound to the oxide components of the catalysts was observed. In the absence of water, these species accumulated on the catalyst surface and exhibited high thermal stability. The surface-bound NCO species reacted readily with H_2O to form the hydrolysis products of NH_3 and CO_2. The NH_3 thus produced then could react with NO_x to form an intermediate that eventually decomposes to give N_2 and H_2O. Removing NO_x from the $Pt/BaO/Al_2O_3$ catalyst was very effective when both H_2 and CO were used as reducing agents; the rate of removal was lower than that in the presence of only H_2 but higher than that in presence of only CO. At low temperatures, H_2 was the primary reducing agent. At high temperatures, NCO can react directly with NO_x to form N_2 and CO_2, whereas at intermediate temperatures, water, formed in the reduction with H_2, can hydrolyze NCO to form the intermediate that eventually decomposes to N_2 and H_2O.

Acknowledgments

Financial support was provided by the US Department of Energy (DOE), Office of Freedom Car and Vehicle Technologies. The work was performed in the Environmental Molecular

Sciences Laboratory (EMSL) at the Pacific Northwest National Laboratory (PNNL). The EMSL is a national scientific user facility supported by the DOE Office of Biological and Environmental Research. PNNL is a multiprogram national laboratory operated for the DOE by Battelle Memorial Institute under contract DE-AC06-76RLO 1830. The work at Brookhaven National Laboratory was financed through contract DE-AC02-98CH10086 with the DOE Division of Chemical Sciences.

References

[1] S. Yoon, A.G. Panov, R.G. Tonkyn, A.C. Ebeling, S.E. Barlow, M.L. Balmer, Catal. Today 72 (2002) 243.
[2] H. Bosch, F. Janssen, Catal. Today 2 (1988) 369.
[3] R. Burch, Catal. Rev.-Sci. Eng. 46 (2004) 271.
[4] P.L.T. Gabrielsson, Top. Catal. 28 (2004) 177.
[5] E. Fridell, H. Persson, B. Westerberg, L. Olsson, M. Skoglundh, Catal. Today 66 (2000) 71.
[6] T. Lesage, C. Verrier, P. Bazin, J. Saussey, M. Daturi, Phys. Chem. Chem. Phys. 5 (2003) 4435.
[7] M.L. Unland, J. Phys. Chem. 77 (1973) 1952.
[8] P. Jozsa, E. Jobson, M. Larsson, Top. Catal. 30/31 (2004) 177.
[9] S. Poulston, R.R. Rajaram, Catal. Today 81 (2003) 603.
[10] D. James, E. Fourre, M. Ishii, M. Bowker, Appl. Catal. B: Environ. 45 (2003) 147.
[11] N.W. Cant, M.J. Patterson, Catal. Lett. 85 (2003) 153.
[12] J. Szanyi, J.H. Kwak, D.H. Kim, S.D. Burton, C.H.F. Peden, J. Phys. Chem. B 109 (1) (2005) 27.
[13] Ch. Sedlmair, K. Seshan, A. Jentys, J.A. Lercher, J. Catal. 214 (2003) 308.
[14] B. Westerberg, E. Fridell, J. Mol. Catal. A: Chem. 165 (2001) 249.
[15] L. Olsson, E. Fridell, J. Catal. 210 (2002) 340.
[16] J. Szanyi, J.H. Kwak, D.H. Kim, J. Hanson, C.H.F. Peden, manuscript in preparation.
[17] K.I. Hadjiivanov, Catal. Rev.-Sci. Eng. 42 (1&2) (2000) 71.
[18] N. Bion, J. Saussey, C. Hedouin, T. Seguelong, M. Daturi, Phys. Chem. Chem. Phys. 3 (2001) 4811.
[19] M. Haneda, Pusparatu, Y. Kintaichi, I. Nakamura, M. Sasaki, T. Fujitani, H. Hamada, J. Catal. 229 (2005) 197.
[20] H. Arai, H. Tominaga, J. Catal. 43 (1976) 131.
[21] F. Prinetto, G. Ghiotti, I. Nova, L. Lietti, E. Tronconi, P. Forzatti, J. Phys. Chem. B 105 (2001) 12732.
[22] I. Nova, L. Castoldi, L. Lietti, E. Tronconi, P. Forzatti, F. Prinetto, G. Ghiotti, J. Catal. 222 (2004) 377.
[23] P. Broquist, H. Gronbeck, H. Fridell, I. Panas, J. Phys. Chem. B 108 (2004) 3523.
[24] P.T. Fanson, M.R. Horton, W.N. Delgass, J. Lauterbach, Appl. Catal. B 46 (2004) 393.
[25] W.S. Epling, J.E. Parks, G.C. Campbell, A. Yezerets, N.W. Currier, L.E. Campbell, Catal. Today 96 (2004) 21.
[26] K. Taylor, Catal. Rev.-Sci. Eng. 3 (1993), and references therein.
[27] B. Frank, G. Emig, A. Renken, Appl. Catal. B: Environ. 19 (1998) 45.
[28] G. Pirug, H.P. Bonzel, J. Catal. 50 (1977) 64.
[29] T.M. Salama, R. Ohnishi, T. Shido, M. Ichikawa, J. Catal. 162 (1996) 169.
[30] N. Macloed, R.M. Lambert, Chem. Commun. (2003) 1300.

Further reading

[1] F. Solymosi, L. Völgyesi, J. Sárkány, J. Catal. 54 (1978) 336.